



HAL
open science

High-resolution repertoire analysis reveals a major bystander activation of Tfh and Tfr cells

Paul-Gydeon Ritvo, Ahmed Saadawi, Pierre Barennes, Valentin Quiniou, Wahiba Chaara, Karim El Soufi, Benjamin Bonnet, Adrien Six, Mikhail Shugay, Encarnita Mariotti-Ferrandiz, et al.

► **To cite this version:**

Paul-Gydeon Ritvo, Ahmed Saadawi, Pierre Barennes, Valentin Quiniou, Wahiba Chaara, et al.. High-resolution repertoire analysis reveals a major bystander activation of Tfh and Tfr cells. Proceedings of the National Academy of Sciences of the United States of America, 2018, 115 (38), pp.9604-9609. 10.1073/pnas.1808594115 . hal-03867773

HAL Id: hal-03867773

<https://hal.sorbonne-universite.fr/hal-03867773v1>

Submitted on 24 Feb 2023

HAL is a multi-disciplinary open access archive for the deposit and dissemination of scientific research documents, whether they are published or not. The documents may come from teaching and research institutions in France or abroad, or from public or private research centers.

L'archive ouverte pluridisciplinaire **HAL**, est destinée au dépôt et à la diffusion de documents scientifiques de niveau recherche, publiés ou non, émanant des établissements d'enseignement et de recherche français ou étrangers, des laboratoires publics ou privés.



Distributed under a Creative Commons Attribution - NonCommercial - NoDerivatives 4.0 International License



High-resolution repertoire analysis reveals a major bystander activation of Tfh and Tfr cells

Paul-Gydeon Ritvo^a, Ahmed Saadawi^{a,1}, Pierre Barennes^{a,1}, Valentin Quiniou^{a,b,1}, Wahiba Chaara^{a,b}, Karim El Soufi^a, Benjamin Bonnet^a, Adrien Six^{a,b}, Mikhail Shugay^{c,d,e}, Encarnita Mariotti-Ferrandiz^{a,b}, and David Klatzmann^{a,b,2}

^aImmunology-Immunopathology-Immunotherapy Laboratory, UMR_S 959, INSERM, Sorbonne Université, F-75005 Paris, France; ^bBiotherapy Unit, Inflammation-Immunopathology-Biotherapy Department, Hôpital Pitié-Salpêtrière, Assistance Publique-Hôpitaux de Paris, F-75013 Paris, France; ^cCenter for Data-Intensive Biomedicine and Biotechnology, Skolkovo Institute of Science and Technology, 143026 Moscow, Russia; ^dDepartment of Molecular Technologies, Pirogov Russian National Research Medical University, 117997 Moscow, Russia; and ^eImmunosequencing Algorithms Group, Institute of Bioorganic Chemistry, Russian Academy of Sciences, 117997 Moscow, Russia

Edited by Philippa Marrack, National Jewish Health, Denver, CO, and approved July 30, 2018 (received for review May 21, 2018)

T follicular helper (Tfh) and regulatory (Tfr) cells are terminally differentiated cells found in germinal centers (GCs), specialized secondary lymphoid organ structures dedicated to antibody production. As such, follicular T (Tfol) cells are supposed to be specific for immunizing antigens, which has been reported for Tfh cells but is debated for Tfr cells. Here, we used high-throughput T cell receptor (TCR) sequencing to analyze the repertoires of Tfh and Tfr cells, at homeostasis and after immunization with self- or foreign antigens. We observed that, whatever the conditions, Tfh and Tfr cell repertoires are less diverse than those of effector T cells and Treg cells of the same tissues; surprisingly, these repertoires still represent thousands of different sequences, even after immunization with a single antigen that induces a 10-fold increase in Tfol cell numbers. Thorough analysis of the sharing and network of TCR sequences revealed that a specific response to the immunizing antigen can only, but hardly, be detected in Tfh cells immunized with a foreign antigen and Tfr cells immunized with a self-antigen. These antigen-specific responses are obscured by a global stimulation of Tfh and Tfr cells that appears to be antigen-independent. Altogether, our results suggest a major bystander Tfol cell activation during the immune response in the GCs.

diversity | autoimmunity | stochasticity | TCR | follicular

The germinal center (GC) is an essential structure for the activation of B cells and the production of high-affinity antibodies (1, 2). In GCs, T follicular helper (Tfh) cells promote the differentiation and activation of B cells into plasma cells (3, 4). In contrast, the recently discovered T follicular regulatory (Tfr) cells inhibit antibody production (5–7).

Several studies based on peptide class II MHC tetramers (8, 9) or enzyme-linked immunospot assays (10) established that Tfh cells are specific for peptides of the immunizing antigen. Actually, it is believed that to activate B cells, Tfh cells must recognize the same antigen as the B cells they help (11, 12). In contrast, contradictory results have been obtained regarding the antigen specificity of Tfr cells. The Tfr cell repertoire has been studied after immunization with the myelin oligodendrocyte glycoprotein (MOG) in wild-type and MOG knockout mice, for which MOG is a self- or foreign antigen, respectively. In both conditions, tetramer-positive Tfr cells specific for the immunodominant peptide of MOG were identified (13). In this study, it was also shown that Tfh and Tfr cells share similar T cell receptors (TCRs) specific for the immunizing antigen (13). In contrast, we reported oligoclonal expansions in Tfh cells and broad TCR usage in Tfr cells of mice immunized with a foreign antigen (14). However, these results (13, 14) were obtained using CD4⁺CXCR5^{hi}PD1^{hi}Foxp3⁺CD25⁺ “Tfr” cells, while we and others recently showed that bona fide Tfr cells are CD25[−] (15–17). Therefore, the observed TCR repertoire diversity and composition from these studies were probably those of a mixture of TCRs derived from Treg and Tfr cells.

In these previous studies, it should also be noted that Tfh and Tfr cell specificity was studied either (*i*) in cells purified with tetramers, purposely assessing only limited specificities (13), or (*ii*) using high-throughput sequencing (HTS) in TCR-transgenic mice

with a biased repertoire (14). Therefore, the study of the Tfh and Tfr cell TCR repertoire remains to be performed in unmanipulated mice and using better characterized cell populations for Tfr cells.

Here, we stringently purified CD4⁺PD1^{hi}CXCR5^{hi}Foxp3⁺CD25[−] Tfr cells from wild-type mice and compared their TCR repertoires with those of Tfh, Treg, and effector T (Teff) cells by HTS targeting the TCR β-chain. Cells were obtained at homeostasis or from mice immunized either with a self-antigen [insulin (INS)] or a foreign antigen [ovalbumin (OVA)]. Our work reveals an unexpected high diversity of the repertoire of follicular T (Tfol) cells suggestive of a bystander activation during antigen-specific responses.

Results

Mice with the transgenic expression of GFP under the promoter of Foxp3 were used to purify Tfh (CD4⁺CD8[−]CXCR5^{hi}PD1^{hi}GFP[−]), Tfr (CD4⁺CD8[−]CXCR5^{hi}PD1^{hi}CD25[−]GFP⁺), Teff (CD4⁺CD8[−]CXCR5^{lo}PD1^{lo}GFP[−]), and Treg (CD4⁺CD8[−]CXCR5^{lo}PD1^{lo}GFP⁺) cells. To recover sufficient amounts of the scarce Tfr cells, we purified cells from pools of six to eight mice (these “Metamice” are henceforth referred to as “Mice”). We generated three pools of mice immunized i.p. with OVA in alum, three pools of mice immunized with INS in alum, and two pools that were not immunized. Spleen histology showed that there are already

Significance

T follicular helper (Tfh) cells promote high-affinity antibody production by B cells, while T follicular regulatory (Tfr) cells repress it. Deciphering Tfh and Tfr cell specificity should illuminate the understanding of how antibody responses are regulated. We analyzed the T cell receptor repertoire of Tfh and Tfr cells from wild-type mice, immunized or not. This showed that Tfr cells respond to self-antigens, while Tfh cells respond to foreign antigens. Importantly, these specific responses were obscured by an important bystander activation of follicular T cells. We think and discuss that this bystander activation has a general significance for immune responses and possibly for immunopathologies.

Author contributions: P.-G.R., E.M.-F., and D.K. designed experiments; P.-G.R., V.Q., and B.B. performed experiments; P.-G.R., A. Saadawi, P.B., W.C., K.E.S., A. Six, M.S., E.M.-F., and D.K. analyzed data; P.-G.R., E.M.-F., and D.K. wrote the paper; and D.K. conceived, supervised, and obtained funding for the entire study.

The authors declare no conflict of interest.

This article is a PNAS Direct Submission.

Published under the PNAS license.

Data deposition: The raw sequences presented in this study have been submitted as a National Center for Biotechnology Information BioProject (ID PRJNA486323) in the Sequence Read Archive, www.ncbi.nlm.nih.gov/sra (accession nos. SAMN09843511–SAMN09843539).

¹A. Saadawi, P.B., and V.Q. contributed equally to this work.

²To whom correspondence should be addressed. Email: david.klatzmann@sorbonne-universite.fr.

This article contains supporting information online at www.pnas.org/lookup/suppl/doi:10.1073/pnas.1808594115/-DCSupplemental.

Published online August 29, 2018.

detectable GCs at homeostasis, which increase in number and size after immunization (*SI Appendix, Fig. S1*).

Tfol Cells Have a Lower Diversity than Non-Tfol Cells. We first analyzed the TCR diversity of the four cell subsets in the three immunization settings. The numbers of sequences representing a unique combination of TRBV-complementarity-determining region 3p (CDR3p)-TRBJ (uTR-B) obtained for each sample are provided in *SI Appendix, Table S1*. Rarefaction curves (Fig. 1*A*), which represent the observed numbers of different uTR-Bs at a given sample size (i.e., number of sequences), showed that both Tfr and Tfh cell repertoires are less diverse than those of T_{eff} and Treg cells in nonimmunized mice (*Left*) and mice immunized with either INS (*Middle*) or OVA (*Right*). Other commonly used diversity indices confirmed these observations. The percentage of the most predominant uTR-Bs that account for 50% of the sequences of a sample size (P50) of Tfol cells is significantly lower than the average P50 of T_{eff} and Treg cell repertoires (Fig. 1*B*). The Pielou index (18), which assesses the evenness of a repertoire, is significantly lower for Tfol cells compared with non-Tfol cells (Fig. 1*C*).

The lower richness described by the rarefaction curves and the P50 index could be explained by a higher number of expansions among Tfol cells compared with non-Tfol cells (Fig. 1*D*). The 250 predominant uTR-Bs for Tfr and Tfh cells represent at least 20% of the total repertoire, compared with around 5% for T_{eff} and Treg cells. Some uTR-Bs represent more than 1% of the total number of sequences in Tfr and Tfh cell samples, which is not observed in Treg and T_{eff} cells. Finally, reconstruction of immunoscope profiles (19) from next-generation sequencing data highlight a Gaussian distribution profile for T_{eff} and Treg cells, and numerous expansions in Tfol cell samples (*SI Appendix, Fig. S2*). Altogether, these results suggest that the global characteristics of the Tfh and Tfr cell repertoires are similar and that both subsets have a skewed diversity compared with non-Tfol cells.

TRBVBJ Gene Usage and uTR-B Composition Are Different in the Four Cell Populations. A principal component analysis (PCA) of TRBVBJ combination frequencies (Fig. 2*A*) separates Tfol from non-Tfol

cells very well, showing clear different usage of TRBV and TRBJ combinations in the two groups, with the first principal component (PC1) explaining more than 65% of the variability. These results are in agreement with the Morisita-Horn similarity indices computed for TRBVBJ usage between each pair of samples (Fig. 2*B*).

We further explored diversity at the uTR-B level, using the frequency of uTR-Bs shared by at least seven samples to reduce noise due to private uTR-Bs. Tfol cells are well separated from non-Tfol cells on PC1 (22%). Tfh and Tfr cells are remarkably close to each other, in contrast to T_{eff} and Treg cells (Fig. 2*C*). The Morisita-Horn index computed for those uTR-Bs also showed that T_{eff} and Treg cluster together, apart from the Tfh and Tfr subsets (Fig. 2*D*). Strikingly, at the uTR-B level, Tfr and Tfh cell similarity is very low, suggesting that their repertoire might be different.

Tfr and Tfh Cells Have Distinct Repertoires. We next compared the uTR-B composition of Tfr and Tfh cell repertoires irrespective of the immunization. As illustrated in *SI Appendix, Fig. S3*, we first ordered all uTR-Bs of a given Tfr cell sample by decreasing frequency and selected the 250 predominant uTR-Bs. We then calculated the frequency of these 250 uTR-Bs in each of the seven other Tfr cell samples and among the seven Tfh cell samples from the remaining Mice. For each cell subset, the average frequency of the seven values was calculated. This procedure was repeated with the 250 top uTR-Bs of each subset. Fig. 3*A* shows the summary graph with the average frequency for each of the eight samples plotted per cell subset. We used the same methodology to analyze the predominant Tfh uTR-Bs (Fig. 3*B*). The results showed that, irrespective of immunization, uTR-Bs found predominantly in one Tfr cell sample are also found in higher proportions in other Tfr cell samples than in Tfh cell samples (Fig. 3*A*). Conversely, uTR-Bs predominantly found in one Tfh cell sample are mostly shared with other Tfh cell samples rather than with Tfr cell samples (Fig. 3*B*).

We then performed a similar analysis to compare the response to the specific immunizations. The 250 predominant uTR-Bs of each of the Tfr cell samples from Mice immunized with INS were sought (*i*) in the two other Tfr samples of either INS- or OVA-immunized Mice, generating six and nine values per condition,

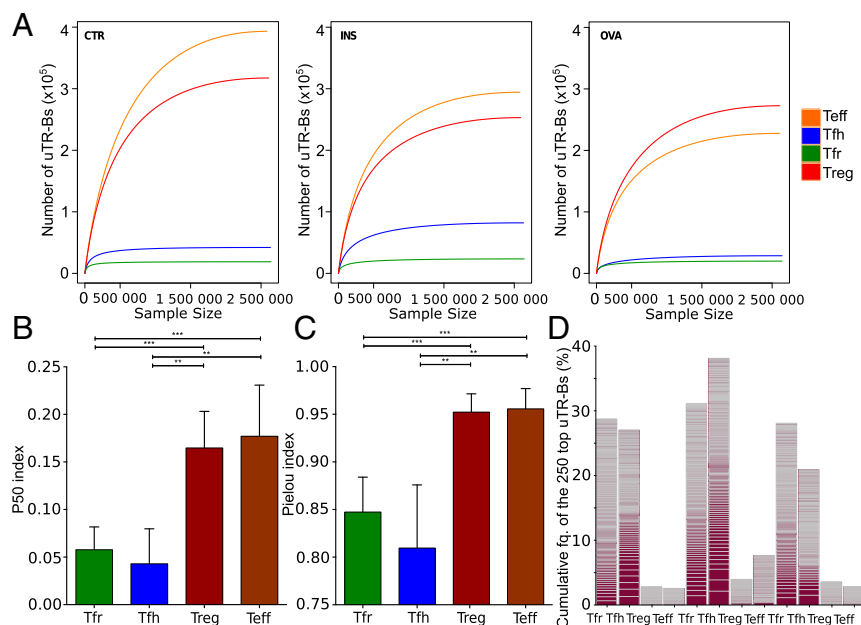


Fig. 1. Tfol cells display a lower diversity than non-Tfol cells, yet are polyclonal. (*A*) Representative rarefaction curves displaying the number of uTR-Bs as a function of the number of reads (sample size) from nonimmunized control (CTR) Mice (*Left*) and Mice immunized with either INS (*Middle*) or OVA (*Right*). P50 (*B*) and Pielou's evenness (*C*) indices were calculated for all of the samples of each T cell subset (details are provided in *SI Appendix, Table S1*) and compared by the Mann-Whitney *U* test (**P* < 0.05; ***P* < 0.01; ****P* < 0.001). (*D*) Cumulative frequencies of the 250 predominant uTR-Bs for each of the four T cell subsets were calculated. One histogram bar represents one sample, and one colored line represents one uTR-B.

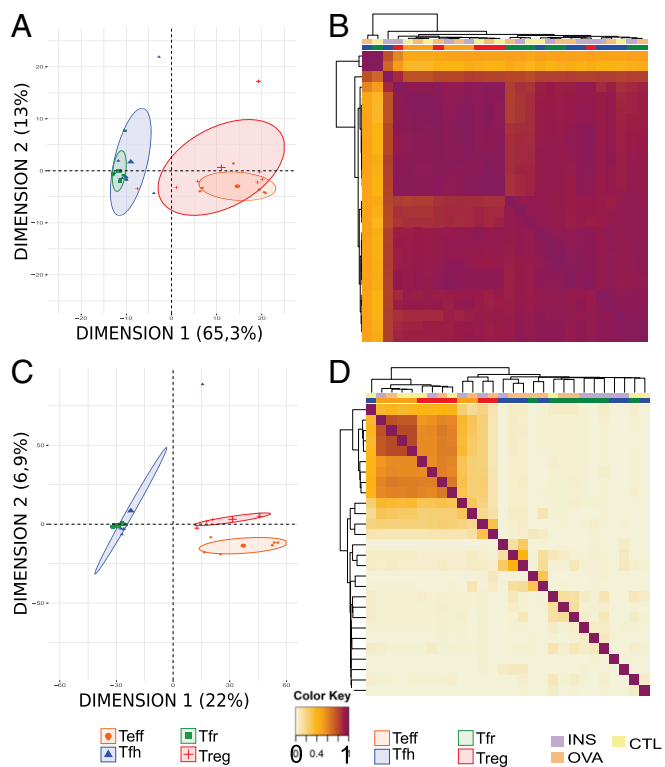


Fig. 2. TRBVBJ gene usage and uTR-B composition separate Tfol cells from non-Tfol cells. (A) PCA projection of the four subset samples according to the first two components (x axis, PC1; y axis, PC2) is plotted for TRBVBJ usage. (B) Hierarchical clustering heat map of Morisita–Horn (MH) similarity index values calculated on TRBVBJ gene usage frequencies for all pairs of samples according to the indicated color scale. (C) PCA is plotted according to the first two components (x axis, PC1; y axis, PC2) using the frequencies of the uTR-Bs shared by at least seven samples across the Tfr, Tfh, Treg, and Teff cells. (D) Hierarchical clustering heat map of MH similarity index values calculated on uTR-B frequencies as in C for all pairs of samples according to the indicated color scale. CTL, control.

respectively, and (ii) in the three other Tfh samples from either INS- or OVA-immunized Mice, generating nine values per condition (Fig. 3C). The same approach was applied to uTR-Bs of Tfr samples from OVA-immunized Mice (Fig. 3E). We found that frequent uTR-Bs from Tfr cells of INS-immunized Mice are present in higher proportions in Tfr cell samples from INS-immunized Mice than in other cell subsets or immunization conditions (Fig. 3C); this was not true for uTR-Bs of Tfr cells from OVA-immunized Mice (Fig. 3E). Conversely, Tfh cell major uTR-Bs after INS immunization were similarly found in Tfh cells regardless of the immunizing antigen (Fig. 3D), while those detected after OVA immunization were more shared in Tfh cells from OVA-immunized Mice. It is of note that Tfr predominant clonotypes from immunized mice (either INS or OVA) can also be detected in Tfr cells from nonimmunized mice (Fig. 3C and E), while Tfh major clonotypes from immunized mice are barely shared with Tfh cells from nonimmunized mice (Fig. 3D and F). These results suggest that both Tfr and Tfh major responses are biased, respectively, toward self- and foreign antigens.

We further analyzed the specific response to the immunization within the more restricted repertoire of uTR-Bs shared by three similar samples. These “public uTR-Bs” from Tfh samples of OVA-immunized Mice represent an average of 6% of the repertoire of these cells, but less than 2% of the repertoires of the other categories of cells (Tfr cells from all conditions or Tfh cells from Mice immunized with INS or nothing) (Fig. 4A). In contrast, public uTR-Bs from Tfh cells of INS-immunized Mice were equally represented among all samples, amounting to 2% of their

repertoire (Tfh and Tfr cells, irrespective of the immunization) (Fig. 4B). Conversely, for Tfr cells, there was threefold higher uTR-B sharing between Tfr cells from Mice immunized with INS than for Mice immunized with OVA (Fig. 4C and D).

Exploring the Immune Response to Immunization by uTR-B Clustering.

As the specific response of Tfr and Tfh cells was, surprisingly, hardly detectable at the stringent level of uTR-Bs, we analyzed it at the level of CDR3 clusters of proximate uTR-Bs, within the first 1,000 predominant CDR3s (20) obtained after pooling the top 1,000 CDR3s of each sample per condition to focus on the most representative CDR3s (Fig. 5). CDR3s are represented as a network where each unique CDR3 sequence is a node and is connected to all other nodes that have a Levenshtein distance of 1 (i.e., only one amino acid difference). Teffs and Tregs at homeostasis and after OVA immunization showed similar cluster patterns (Fig. 5A), with six to seven large clusters composed of more than 15 CDR3s and few small clusters or singletons. CDR3 frequency was similarly low (1,000 copies) regardless of belonging to a cluster or not.

Surprisingly, the cluster pattern for Tfol cells (Fig. 5B) was similar at homeostasis and after OVA immunization. Tfh CDR3 networks (Fig. 5B, Top) showed clusters composed of no more than 22 CDR3s, much lower than in Treg and Teff cells, but with much more abundant CDR3s represented by up to >40,000 copies. It is of note that there were also more singletons represented at high copy numbers. Similar observations can be made from Tfr CDR3 networks (Fig. 5B, Bottom), with even fewer and smaller clusters, as well as many nodes with high copy numbers within clusters and in singletons. Similar results for Tfol cell clustering patterns were seen after immunization with INS (*SI Appendix*, Fig. S5).

Inferring Subset- and Treatment-Specific TCR Motifs.

As we could hardly detect specific immune responses with the previous methods, we next applied a TCR neighbor enrichment test (TCRNET) to detect events of convergent recombination and the presence of highly similar TCR sequences that are unlikely to

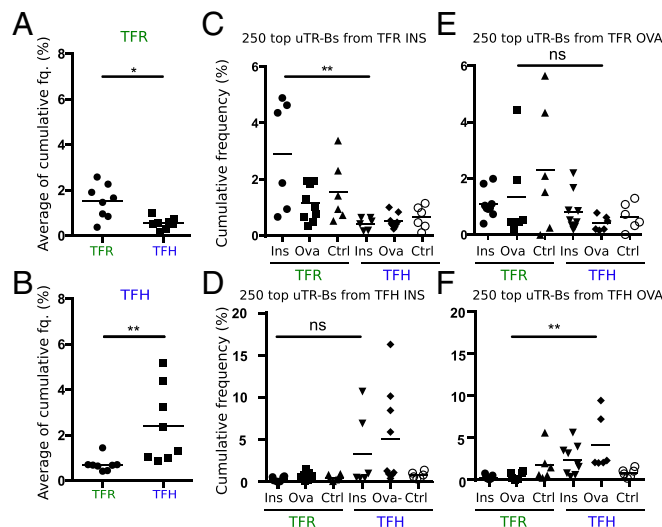


Fig. 3. Tfr and Tfh cell-predominant uTR-Bs are unique to each subset. Average cumulative frequencies calculated for the 250 predominant uTR-Bs of Tfr (A) and Tfh (B) cells. Plots show the average of the predominant Tfr cell uTR-Bs among Tfr and Tfh cell samples of the other seven individuals (A) and of predominant Tfh cell uTR-Bs among Tfr and Tfh cell samples of the other seven individuals (B). Plots show the frequency of the predominant uTR-Bs from Tfr cells (C and E) and Tfh cells (D and F) from INS-immunized (C and D) and OVA-immunized (E and F) Mice among Tfr and Tfh cell samples of the other seven Mice depending on the immunizing antigen. Ctrl, control; ns, not significant.

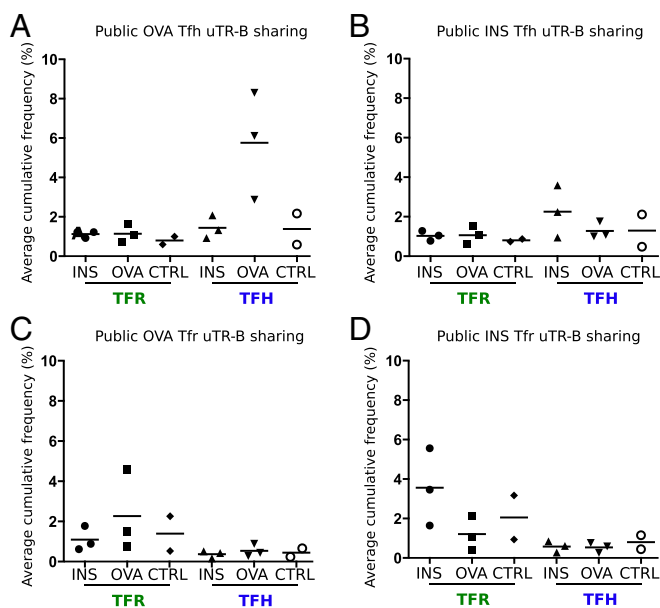


Fig. 4. Tfr and Tfh are specific, respectively, for self-antigen and non-self antigen. Histograms show the averages of cumulative frequencies of predominant uTR-Bs shared by the three Tfh cell subsets across all subsets from Mice immunized with OVA (A) or INS (B), or shared by the three Tfr subsets across all subsets from Mice immunized with OVA (C) or INS (D). CTRL, control.

be encountered by chance. Briefly, we measured the number of V(D)J recombination events in a given sample and compared it with the number expected from a metadataset that is a pool of all TCR sequences from all samples; this detects “core” uTR-Bs enriched in highly similar neighbor sequences and around which uTR-B sequence clusters are built (Fig. 6).

The abundance of enriched clusters varied substantially across samples, with a higher abundance in Tfh and Tfr cells than in Teff and Treg cells (Fig. 6A). Interestingly, the heat map of scaled uTR-B cluster abundances (Fig. 6B) showed sets of clusters that are both highly abundant and “private” to Tfh and Tfr cell samples from immunized Mice, while no such observations were made for Teff and Treg cell samples. The representative uTR-B cluster motifs and networks shown in Fig. 6C display degenerate motifs for clusters that are private to Tfr-INS and Tfh-OVA responses. On the other hand, “public” Tfr/Tfh responses to both INS and OVA, as well as Tfr/Tfh

clusters detected in controls, were all characterized by diverse networks and fewer informative motifs.

Discussion

Tfh and Tfr Cells Have a Higher TCR Diversity than Expected, and Specific Responses to Immunization Can Hardly Be Detected. Tfol cell TCR repertoires are less diverse than those of non-Tfol cells (Fig. 1), but still surprisingly diverse. Indeed, these cells that expand in response to immunization are stringently identified (15) by markers that assign them to the GCs, specialized sites in which antigen-specific antibodies are formed (2). It is thought that antigen-specific B cells act as antigen-presenting cells (APCs) for Tfh cells in the GCs, implying that B cells and the Tfh cells should be specific for the same antigen (11, 12). It could thus be conjectured that Tfh cells that are responding to an immunization would have a repertoire limited to a few uTR-Bs, with large expansions. Instead, we found thousands of sequences in every Tfh and Tfr cell sample (Fig. 1), a point that was missed by analyzing Tfh cells purified using tetramers (13) or from mice bearing a TCR- β fixed chain (14).

Moreover, the evidence for a specific response to the immunizing antigens is weak. Despite a major increase in the number of Tfh and Tfr cells after an immunization, the repertoires of Tfol cells at homeostasis or after activation were rather similar. At the clonotypic level, the representation of the 250 most frequently expressed uTR-Bs was very similar with or without immunization (Fig. 1D).

Tfh Cells Predominantly Respond to Foreign Antigens, While Tfr Cells Respond to Self-Antigens.

Independent of the immunization, the predominant uTR-Bs of Tfr cells in Mice are systematically found at higher frequencies in Tfr cells of other individuals than in Tfh cells and, inversely, for Tfh cell-predominant uTR-Bs. This confirms previous observations that Tfh and Tfr cells somehow have different repertoires (14). Taking immunization into consideration, sharing of predominant uTR-Bs suggests that the Tfh cell response is mostly toward foreign antigens, while the Tfr cell response is mostly toward self-antigens. This is in agreement with our recent observation that Tfr cells increase significantly more in INS-immunized compared with OVA-immunized animals (15), and with a recent study showing that Tfr cells have an effect only on self-reactive antibody responses (17). This observation will have to be extended to other self-antigens and non-self antigens.

The Tfol Cell Compartment Results, in Large Part, from a Major Bystander Activation.

The number of Tfh cells increases \sim 10-fold after immunization with OVA (15). If this had corresponded to an expansion of antigen-specific Tfh cells, it should have led to the detection of a limited number of highly expanded uTR-Bs, which

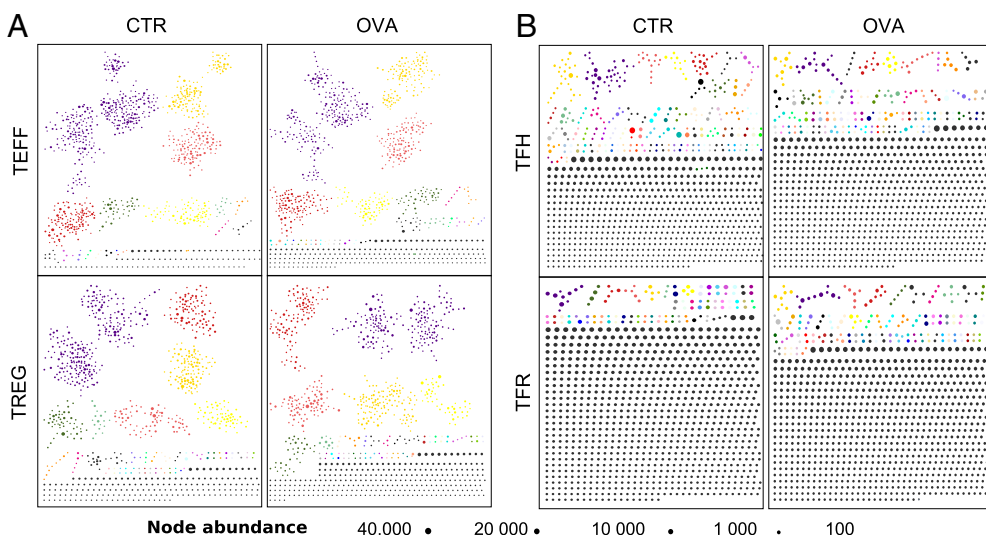


Fig. 5. Networks of the top 1,000 CDR3 amino acid (AA) sequences for follicular (Tfol) and nonfollicular T cells in control (CTR) vs. OVA immunization. Treg and Teff (A) and Tfh and Tfr (B) networks are formed by the merged top 1,000 CDR3 AA sequences in the uTR-B repertoire from nonimmunized (Left) and OVA-immunized (Right) Mice. Nodes (CDR3 AA sequences) were connected by edges if a Levenshtein distance of 1 (one AA insertion/substitution/deletion) existed. Node size indicates its abundance (abundance scale below). A cluster was defined as a set comprising a minimum of two nodes and one edge. Each cluster had a unique random color, while singletons had a black color.

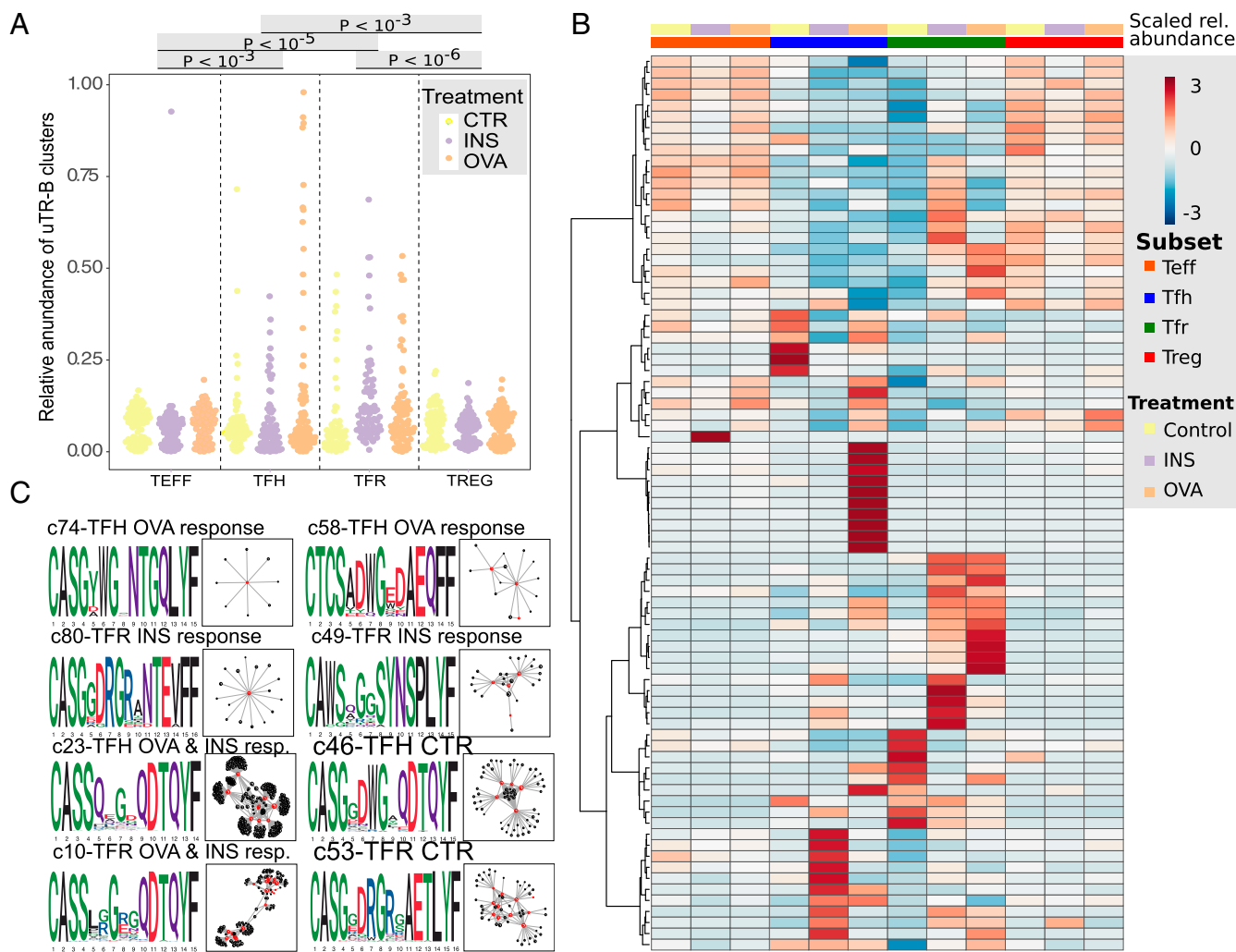


Fig. 6. Analysis of clusters obtained using the TCRNET. (A) Swarm plots of relative abundances of TCR clusters. Relative abundances for each cluster are calculated by computing the sum of TCR uTR-B frequencies in each sample (pooled samples for each treatment and subset are used) and dividing them by the sum over all samples. ANOVA shows a significant association of relative abundances with subset ($F = 14$, $P < 10^{-8}$), treatment ($F = 4$, $P < 0.05$), and their interaction ($F = 4$, $P < 0.001$). P values of the post hoc Tukey test for subsets are shown above the plot. CTR, control. (B) Heat map of scaled TCR cluster abundances. Abundances are scaled to have zero mean and unit SD for each pooled sample. The dendrogram above the heat map is computed using hierarchical clustering (Ward method). rel., relative. (C) Representative TCR CDR3 sequence logos and graphs for selected clusters. Graph nodes are scaled according to the mean TCR uTR-B frequency across all samples. Red nodes represent core TCR uTR-Bs selected by TCRNET.

is clearly not observed. Rather, in Tfol cells, the 1,000 most frequently represented uTR-Bs are expanded (mean of 1,000 copies/clonotypes) compared with non-Tfol cells (mean of 200 copies/clonotypes), including those that are not part of clusters (Fig. 5). This suggests that the overall expansion of Tfol cells after immunization results, in part, from the expansion of cells that are not responding to immunizing epitopes (or to proteins from the adjuvant, as we used alum). This suggests that the initial trigger of the immune response, provided by dendritic cells, could activate not only high-affinity, antigen-specific Tfh cells (8) but also bystander T cells with specificity for other antigens presented by these dendritic cells and/or activated under the effects of the cytokine environment. In this way, this bystander activation could be related to the major role of IL-1 in Tfh cell activation that we recently reported (15). Alternatively, or complementarily, the very high cross-reactivity of single TCRs (21), which have been suggested to recognize thousands of different peptides (22), could explain the bystander activation of cells bearing promiscuous TCRs with low affinity for the immunizing antigen, which are therefore less strongly stimulated and not driven to proliferate highly.

Similarly, our results show that Tfr cell repertoire diversity is high, regardless of the nature of the immunizing antigen. This bystander effect for Tfr activation is less unexpected as, even in the context of a specific immunization, many other self-antigens are expressed by APCs.

The Repertoire of Tfol Cells at Homeostasis. Surprisingly, there are already numerous GCs in the spleen from unimmunized mice (*SI Appendix, Fig. S1*), and the repertoire of Tfol cells from these is remarkably similar to the one seen after immunization, comprising small clusters but also single uTR-Bs with quite large expansions. It is not known to which stimuli these GCs respond or whether the 10-fold increase in Tfol cell numbers after immunization reflects/comprises an expansion of Tfol cells from preexisting GCs, which could explain, in part, the difficulties in detecting a specific immune response to the immunizing antigens. TCR sequencing of Tfol cells from single GCs should help address this question.

In any case, our observations uncover a bystander activation of Tfol cells that we think could reflect a general phenomenon in the T cell response to antigens. Indeed, this bystander effect could only be evidenced because follicular cells (*i*) are terminally differentiated cells found in a highly specialized structure that should

contain only cells responding to the immunization and (ii) can be unambiguously identified and purified. We think that bystander activation during specific immune responses could be a second “immunologist’s dirty little secret” (23). Indeed, immunologists are more reductionist than holistic in their research. We focus on antigen-specific responses, ignoring that the few antigen-specific cells we analyze (i.e., those that are tetramer-positive) are lost in an ocean of cells with unknown specificities. It is now becoming clearer that, in addition to specificity, there is an extraordinary fuzziness and plasticity in the immune system (24). It should be remembered that the specific component of T cell activation is mediated by a receptor that can, in fact, recognize thousands of different peptides, and that the second signals needed for full activation can be provided by many different receptor/ligand interactions that are not specific. The resulting stochasticity in the immune response could have important consequences. Actually, autoantibodies are found in healthy humans and mice in the absence of an immunization with their target antigens (25). It is now important to study whether the bystander activation (of T_H1 cells) has relevance for the development of immunopathologies.

Materials and Methods

Mice, Immunization, and Cell Sorting. Mice, immunization, and cell sorting are described by Ritvo et al. (15) and in *SI Appendix*. All experiments have been performed in agreement with current European legislation on animal care, housing, and scientific experimentation (agreement number A751315). All procedures were approved by the local animal ethics committee from Centre d’Experimentation Fonctionnelle of Sorbonne Université.

TCR Deep Sequencing and Data Processing. RNA from sorted cells was extracted using an RNAqueous kit (Ambion) and processed by iRepertoire following that company’s protocol (25) (*SI Appendix*). Raw data were processed using MiXCR (26) as described in *SI Appendix*.

Data Analysis. Statistical comparisons and multivariate analyses (PCA and hierarchical clustering) were performed using R software, version 3.1.3 (www.r-project.org). The Morisita–Horn index (26) assesses the similarity between sample sets. It ranges from 0 (no common species between the two samples) to 1 (all species are equally present in the two samples). Unlike the Morisita index, the Morisita–Horn variant takes into account the relative abundance of species in the sample. P50 was calculated as the percentage of unique predominant uTRB-Rs necessary to reach 50% of the total number of sequences in a given sample. The Pielou index (18), ranging from 0 to 1, assesses the evenness of a repertoire: The higher the index, the more equally represented the uTRB-Rs are.

Statistical analyses were performed using the nonparametric Mann–Whitney *U* test on GraphPad Prism v5 [*P* values are indicated in the figures, such as nonsignificant (*P* > 0.05), **P* < 0.05, ***P* < 0.01, and ****P* < 0.001].

Network Analysis and Visualization. The most abundant 1,000 CDR3 amino acid sequences were obtained from each pooled cell subset from nonimmunized and OVA-immunized mice. Each CDR3 amino acid sequence represented a node. Nodes were connected if a Levenshtein distance of 1 (one amino acid insertion/substitution/deletion) existed. A cluster was defined as a set with a minimum of two nodes and one edge. Data analysis was performed using Python programming language (<https://www.python.org/>; version 3.6; Python Software Foundation). We used the following packages: Pandas (27) for data preparation, NetworkX (28) to create network objects (gml files) and to obtain node properties (i.e., degree, clustering coefficient, number of clusters, number of edges, number of shared clusters and edges), StringDist (<https://pypi.org/project/StringDist/>) to calculate Levenshtein distances, and seaborn (<https://seaborn.pydata.org/>) to generate figures. All network figures were made using Cytoscape (www.cytoscape.org/) (29). This approach was based on work performed by Madi et al. (20).

Inferring TCR Sequence Clusters and Motifs Using the TCRNET. We infer TCR uTRB-Rs that have an unexpectedly high degree of similar V(D)J rearrangements (neighbors) by comparing the observed number of neighbors in a given sample with the number of neighbors expected from the complete dataset. The neighbor count of a given TCR uTRB-R *d* was computed by counting all nucleotide rearrangements that have the same V and J segments and differ from the uTRB-R by no more than one amino acid substitution in the CDR3 region.

We also computed neighbor count in the control (pooled) dataset *D*, as well as the total number of rearrangements having the same V, J and CDR3 length (*L*) in a given sample *n*, as well as in the control dataset *N*_{VJL}. From these values, we computed the enrichment *P* value using a binomial distribution $p = P_{\text{binom}}(d | D/N_{VJL}, n_{VJL})$. We apply a conservative threshold of *P* < 10⁻⁸ to select enriched TCR uTRB-Rs, roughly equal to 0.05 divided by the total number of uTRB-Rs (10⁶) in the entire dataset.

Data and Materials Availability. The raw sequences presented in this study have been submitted in the National Center for Biotechnology Information Sequence Read Archive (accession nos. SAMN09843511–SAMN09843539).

ACKNOWLEDGMENTS. We thank B. Gouritin and F. Brimaud for help in cell sorting and G. Churlaud for help in experiments. We thank V. Kuchroo for the mice provided. This work has been supported by LabEx Transimmunom (Grant ANR-11-IDEX-0004-02), European Research Council-Advanced Grant “Treg in pathology or disease” (TriPoD) (322856), and Recherche Hospitalo-Universitaire Grant “towards low-dose iL2 market approval for autoimmune diseases” (RHU-iMAP; ANR 16-RHUS-0001). P.-G.R. is an “Ecole de l’Inserm Liliane Bettencourt” doctoral fellow and is sponsored by Servier. M.S. is supported by a Russian Science Foundation Grant (17-15-01495).

- MacLennan IC (1994) Germinal centers. *Annu Rev Immunol* 12:117–139.
- Victoria GD, Nussenzweig MC (2012) Germinal centers. *Annu Rev Immunol* 30:429–457.
- Crotty S (2014) T follicular helper cell differentiation, function, and roles in disease. *Immunity* 41:529–542.
- Vinuesa CG, Linterman MA, Goodnow CC, Randall KL (2010) T cells and follicular dendritic cells in germinal center B-cell formation and selection. *Immunity* 33:72–89.
- Wollenberg I, et al. (2011) Regulation of the germinal center reaction by Foxp3+ follicular regulatory T cells. *J Immunol* 187:4553–4560.
- Chung Y, et al. (2011) Follicular regulatory T (T_{fr}) cells with dual Foxp3 and Bcl6 expression suppress germinal center reactions. *Nat Med* 17:983–988.
- Linterman MA, et al. (2011) Foxp3+ follicular regulatory T cells control T follicular helper cells and the germinal center response. *Nat Med* 17:975–982.
- Fazilleau N, et al. (2007) Lymphoid reservoirs of antigen-specific memory T helper cells. *Nat Immunol* 8:753–761.
- Fazilleau N, McHeyzer-Williams LJ, Rosen H, McHeyzer-Williams MG (2009) The function of follicular helper T cells is regulated by the strength of T cell antigen receptor binding. *Nat Immunol* 10:375–384.
- Leddon SA, Sant AJ (2012) The peptide specificity of the endogenous T follicular helper cell repertoire generated after protein immunization. *PLoS One* 7:e46952.
- Abbas AK, Burstein HJ, Bogen SA (1993) Determinants of helper T cell-dependent antibody production. *Semin Immunol* 5:441–447.
- Lanzavecchia A (1990) Receptor-mediated antigen uptake and its effect on antigen presentation to class II-restricted T lymphocytes. *Annu Rev Immunol* 8:773–793.
- Aloulou M, et al. (2016) Follicular regulatory T cells can be specific for the immunizing antigen and derive from naive T cells. *Nat Commun* 7:10579.
- Maceiras AR, et al. (2017) T follicular helper and T follicular regulatory cells have different TCR specificity. *Nat Commun* 8:15067.
- Ritvo P-G, et al. (2017) T_{fr} cells lack IL-2R α but express decoy IL-1R2 and IL-1Ra and suppress the IL-1-dependent activation of T_H1 cells. *Sci Immunol* 2:eaan0368.
- Wing JB, et al. (2017) A distinct subpopulation of CD25⁺ T-follicular regulatory cells localizes in the germinal centers. *Proc Natl Acad Sci USA* 114:E6400–E6409.
- Botta D, et al. (2017) Dynamic regulation of T follicular regulatory cell responses by interleukin 2 during influenza infection. *Nat Immunol* 18:1249–1260.
- Pielou EC (1966) The measurement of diversity in different types of biological collections. *J Theor Biol* 13:131–144.
- Benveniste O, et al. (2001) Severe perturbations of the blood T cell repertoire in polymyositis, but not dermatomyositis patients. *J Immunol* 167:3521–3529.
- Madi A, et al. (2017) T cell receptor repertoires of mice and humans are clustered in similarity networks around conserved public CDR3 sequences. *eLife* 6:e22057.
- Nelson RW, et al. (2015) T cell receptor cross-reactivity between similar foreign and self peptides influences naive cell population size and autoimmunity. *Immunity* 42:95–107.
- Mason D (1998) A very high level of cross-reactivity is an essential feature of the T-cell receptor. *Immunity Today* 19:395–404.
- Medzhitov R, Janeway CA, Jr (1996) On the semantics of immune recognition. *Res Immunol* 147:208–214.
- Morikawa H, Sakaguchi S (2014) Genetic and epigenetic basis of Treg cell development and function: From a FoxP3-centered view to an epigenome-defined view of natural Treg cells. *Immunity* 40:259–270.
- Quintana FJ, Cohen IR (2004) The natural autoantibody repertoire and autoimmune disease. *Biomed Pharmacother* 58:276–281.
- Horn HS (1966) Measurement of “overlap” in comparative ecological studies. *Am Nat* 100:419–424.
- Rees I (2010) SciPy 2010 - Wes McKinney - pandas and other statistical data analysis tools in Python. Available at <https://archive.org/details/Scipy2010-WesMcKinney-PandasAndOtherStatisticalDataAnalysisToolsIn>. Accessed May 3, 2018.
- Varoquaux G, Vaught T, Millman J (2008) *SciPy 2008: Proceedings of the Seventh Python in Science Conference*. Available at conference.scipy.org/proceedings/scipy2008/SciPy2008_proceedings.pdf. Accessed August 16, 2018.
- Shannon P, et al. (2003) Cytoscape: A software environment for integrated models of biomolecular interaction networks. *Genome Res* 13:2498–2504.